Neutral N−O Chelated Palladium(II) Complexes: Syntheses, Characterization, and Reactivity

Myeongsoon Kang and Ayusman Sen*

Department of Chemistry, The Pennsylvania State University, University Park, Pennsylvania 16802

Received February 22, 2005

A series of neutral salicylaldiminato Pd(II) complexes, Pd(Me)(Ph-CH=N-R′)[3-^{t}Bu-2-(O)-C_6H_3-CH=N-2,6-di-^{i}Pr-C_6H_3] (R = CH_3, *n*-Pr, *tert*-Bu, Ph, benzyl) (**3a**−**3e**) and Pd(Me)[2-(CH=N-*t*-Bu)-Py][3-^{t}Bu-2-(O)C_6H_3-CH=N-2,6-di-^{i}Pr-C_6H_3] (**4**), have been synthesized and characterized. The structures of complexes **3a**, **3c**−**3e**, and **4** have been confirmed by X-ray analysis. NMR studies utilizing **3c** indicate that the insertion of CO into the Pd−Me bond occurs through a five-coordinate intermediate. The acyl compounds in turn undergo imine insertion. The neutral complexes **3a**−**3e** show moderate catalytic activity for the polymerization of methyl acrylate at ambient temperature. However, a radical rather than vinyl insertion mechanism appears to be operative.

Introduction

Since the advent of metallocene-based catalysts for ethene and 1-alkene polymerization,[1,2] much effort has been made to develop metallocene-[3] and nonmetallocene-based[4−7] complexes for the successful homo- or copolymerization of vinyl monomers through successive coordination insertion mechanism. In recent years, the emphasis has been on the development of systems capable of polymerizing polar vinyl monomers, such as acrylates. Because of their tolerance toward functionalities, late transition metal complexes, such as those of palladium and nickel, have been the particular focus of the recent work.[4−8] For the most part, the complexes investigated have been cationic, and while several of them are able to incorporate acrylates in copolymerization reactions, there is a significant attenuation of activity due to coordination of the ester functionality to the metal center.

In view of the observed inhibition of polymerization by polar vinyl monomers for cationic palladium and nickel complexes, attention has turned to the development of less electrophilic, neutral complexes for polymerization of such monomers.[6,7] Recently, several neutral nickel catalysts with [N,O] chelating ligands, modeled after the [P,O] ligands used with SHOP-type catalysts,[9−13] have been reported by DuPont,[14] Grubbs,[15,16] Brookhart,[17−19] and others.[20−22] However, these cause little or no incorporation of acrylates in polymerization reactions. Palladium-based neutral catalysts have also been reported by Novak[23] and Sen.[24] Homopolymerization of methyl acrylate and its copolymerization with 1-alkenes has been achieved. However, a radical rather than vinyl insertion mechanism appears to be operative in these cases.

We report here the synthesis and structural characterization of a series of neutral palladium complexes based on an [N,O] chelating ligand. The reactivity of the complexes toward CO and methyl acrylate is also discussed.

Results and Discussion

Complex Synthesis. The salicylaldimine ligand was prepared by condensation of 3-*tert*-butyl-2-hydroxy-

* To whom correspondence should be addressed. E-mail: asen@psu.edu.

(1) Kaminsky, W.; Arndt, M. *Adv. Polym. Sci.* **1996**, *127*, 143−187.
(2) Brintzinger, H. H.; Fischer, D.; Mulhaupt, R.; Rieger, B.; Waymouth, R. M. *Angew. Chem., Int. Ed. Engl.* **1995**, *34*, 1143−1170.
(3) Alt, H. G.; Koeppl, A. *Chem. Rev.* **2000**, *100*, 1205−1221.
(4) Ittel, S. D.; Johnson, L. K.; Brookhart, M. *Chem. Rev*. **2000**, *100*, 1169−1203.
(5) Britovsek, G. J. P.; Gibson, V. C.; Wass, D. F. *Angew. Chem., Int. Ed.* **1999**, *38*, 428−447.
(6) Mecking, S. *Angew. Chem., Int. Ed.* **2001**, *40*, 534−540.
(7) Gibson, V. C.; Spitzmesser, S. K. *Chem. Rev.* **2003**, *103*, 283−315.
(8) Boffa, L. S.; Novak, B. M. *Chem. Rev.* **2000**, *100*, 1479−1493.
(9) Ostoja-Starzewski, K. A.; Witte, J. *Angew. Chem., Int. Ed. Engl.* **1985**, *24*, 599−601.
(10) Ostoja-Starzewski, K. A.; Witte, J. *Angew. Chem., Int. Ed. Engl.* **1987**, *26*, 63−64.
(11) Klabunde, U.; Ittel, S. D. *J. Mol. Catal.* **1987**, *41*, 123−134.
(12) Klabunde, U.; Mülhaupt, R.; Herskovitz, T.; Janowicz, A. H.; Calabrese, J.; Ittel, S. D. *J. Polym. Sci., Part A: Polym. Chem.* **1987**, *25*, 1989−2003.
(13) Kurtev, K.; Tomov, A. *J. Mol. Catal.* **1994**, *88*, 141−150.
(14) Johnson, L. K.; Bennett, A. M. A.; Ittel, S. D.; Wang, L.; Parthasarathy, A.; Hauptman, E.; Simpson, R. D.; Feldman, J.; Coughlin, E. B. WO 98/30609, 1998.
(15) Wang, C.; Friedrich, S.; Younkin, T. R.; Li, R. T.; Grubbs, R. H.; Bansleben, D. A.; Day, M. W. *Organometallics* **1998**, *17*, 3149−3151.
(16) Younkin, T. R.; Connor, E. F.; Henderson, J. I.; Friedrich, S. K.; Grubbs, R. H.; Bansleben, D. A. *Science* **2000**, *287*, 460−462.
(17) Hicks, F. A.; Brookhart, M. *Organometallics* **2001**, *20*, 3217−3219.
(18) Jenkins, J. C.; Brookhart, M. *Organometallics* **2003**, *22*, 250−256.
(19) Hicks, F. A.; Jenkins, J. C.; Brookhart, M. *Organometallics* **2003**, *22*, 3533−3545.
(20) Rachita, M. J.; Huff, R. L.; Bennett, J. L.; Brookhart, M. *J. Polym. Sci., Part A: Polym. Chem.* **2000**, *38*, 4627−4640.
(21) Dohler, T.; Gorls, H.; Walther, D. *Chem. Commun*. **2000**, 945−946.
(22) Walther, D.; Dohler, T.; Theyssen, N.; Gorls, H. *Eur. J. Inorg. Chem*. **2001**, 2049−2060.
(23) Tian, G.; Boone, H. W.; Novak, B. M. *Macromolecules* **2001**, *34*, 7656−7663.
(24) Elia, C.; Elyashiv-Barad, S.; Sen, A.; Lopez-Fernandez, R.; Albeniz, A. C.; Espinet, P. *Organometallics* **2002**, *21*, 4249−4256.

10.1021/om050126a CCC: $30.25
Publication on Web 06/04/2005

Scheme 1

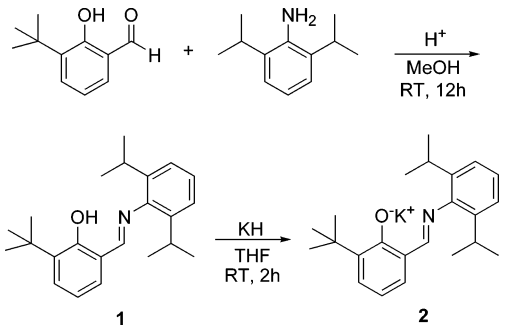

Scheme 2

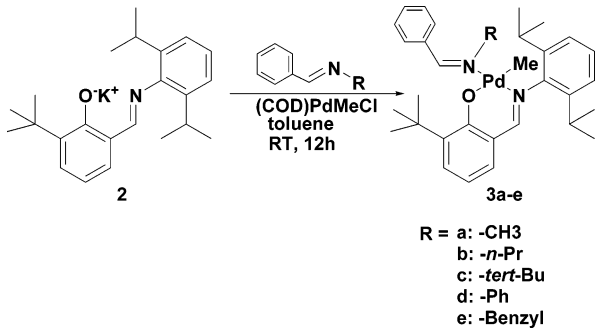

R = a: -CH3
b: -*n*-Pr
c: -*tert*-Bu
d: -Ph
e: -Benzyl

benzaldehyde with 2,6-di-isopropylaniline (Scheme 1). In situ formation of the sodium salt from **1** upon deprotonation with sodium hydride at room temperature, followed by reaction with the palladium precursor, (1,5-cyclooctadiene)palladium(methyl)(chloride), (COD)-Pd(Me)Cl,[25] in toluene was not satisfactory in our case.[15] Only starting ligand was recovered. However, by deprotonation of **1** with a slight excess of potassium hydride in THF, potassium salt **2** as a THF adduct with 1 equiv of THF coordinated was successfully isolated as a yellow solid after triturating with pentane. The potassium salt **2** was relatively stable over the course of several months under a dinitrogen atmosphere.

Neutral palladium complexes **3a**−**3e** (Scheme 2) were first synthesized by combining the potassium salt **2** with (COD)PdMeCl in the presence of a slight excess of an appropriate imine in toluene for ca. 12 h. Potassium chloride was separated by filtration, and the product was isolated by triturating with ether, followed by washing with pentane. Complexes **3a**−**3e** were obtained as yellow solids in yields of ca. 90% upon recrystallization from pentane or methylene chloride/pentane.

For all the complexes, coordination of an imine to the palladium center appears to inhibit the rotation of the 2,6-di-isopropylphenyl group about the N−aryl bond on the NMR time scale and thus renders the individual methyl groups of an isopropyl unit inequivalent in the ^{1}H NMR spectrum. Four doublets, each of which integrates to three protons, are observed. For complex **3e**, two doublets, each of which integrates to one proton, are observed at 5.61 and 5.10 ppm. Clearly, the two methylene protons on the benzyl group (=N-C*H*$_2$-Ph) have different stereochemical environments, which results in the above two sets of doublets. The resonances attributed to the palladium-bound methyl groups are shown at −0.47 to −0.86 ppm, with corresponding ^{13}C NMR resonances at −4.1 to −6.1 ppm.

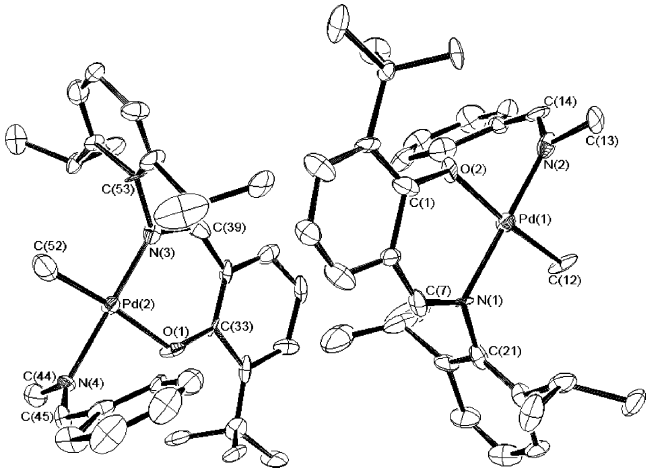

Figure 1. ORTEP view of complex **3a**. Hydrogen atoms are omitted for clarity.

The molecular structures of the complexes **3a** and **3c**−**3e** were determined by single-crystal X-ray structure analysis. X-ray quality crystals of the complexes were obtained either by slow diffusion of pentane into a concentrated solution of **3e** in methylene chloride at room temperature or by cooling a concentrated solution of a complex in pentane to room temperature (**3a** and **3d**) or to −25 °C (**3c**). The ORTEP plots of **3a** and **3c**−**3e** are shown in Figures 1−4 (for crystallographic data, see Table 6 or the Supporting Information for detailed data). The selected bond lengths and angles for **3a** and **3c**−**3e** are given in Tables 1−4. In the solid state they adopt geometries best described as square planar about each palladium center, having slight distortions from idealized geometry. An imine is coordinated through the nitrogen in the *trans* position to the nitrogen of the [N,O] chelate ring. The C−N−C plane including palladium-bound nitrogen of the imine ligand is roughly perpendicular to the square planes around each palladium. The *cis* N−Pd−O angles for the complexes **3a**−**e** exceed 90°, due to the formation of six-membered [N,O] chelate rings. Conversely, the *cis* N−Pd−C angles, containing the imine nitrogen and methyl group, are smaller than 90°.

Complex **4** was prepared to compare the coordinating ability of an imine to pyridine. The reaction of the potassium salt **2** with (COD)PdMeCl in the presence of *tert*-butylpyridin-2-ylmethylene-amine in toluene afforded the target compound **4** as a yellow solid in good yield after removing the solvent under vacuo following filtration. The C*H* imine protons of the monodentate ligand and [N,O] chelate ring show resonances at 7.71 and 9.94 ppm, respectively. The palladium-bound methyl proton resonates at −0.26 ppm. The molecular structure of complex **4** was confirmed by single-crystal X-ray structure analysis. Cooling a concentrated solution of **4** in pentane to room temperature produced a yellow crystal that was suitable for analysis. Figure **5** displays the ORTEP diagram of compound **4**. Selected bond distances and bond angles are collected in Table 5 (see Table 6 for crystallographic data or the Supporting Information for detailed data). In the solid state it shows square planar coordination geometry about palladium, with bond angles slightly deviated from 90° due

(25) Rulke, R. E.; Ernsting, J. M.; Spek, A. L.; Elsevier, C. J.; van Leeuwen, Piet W. N. M.; Vrieze, K. *Inorg. Chem.* **1993**, *32*, 5769−5778.

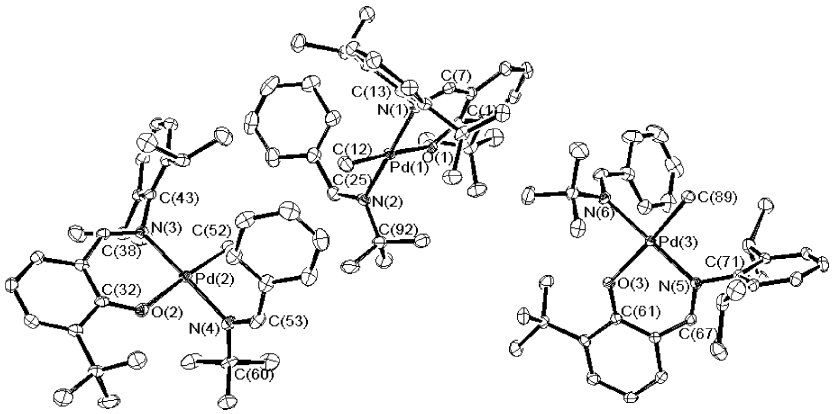

Figure 2. ORTEP view of complex **3c**. Hydrogen atoms are omitted for clarity.

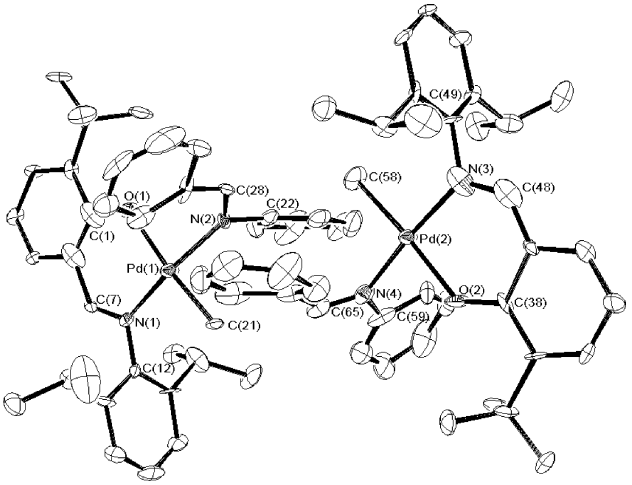

Figure 3. ORTEP view of complex **3d**. Hydrogen atoms are omitted for clarity.

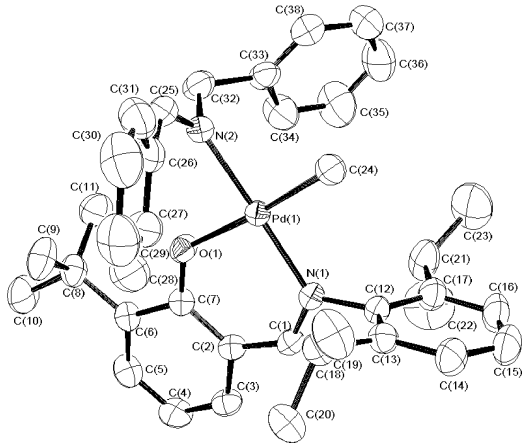

Figure 4. ORTEP view of complex **3e**. Hydrogen atoms are omitted for clarity.

to constraint of the chelate ring. The nitrogen of the pyridine ring rather than that of the imine functionality is bonded to the metal center. Since both nitrogens are sp^2 hybridized, their coordinating abilities might be expected to be similar. On this basis, the observed selectivity can be ascribed to the steric crowding around the imine nitrogen due to the neighboring *tert*-butyl group. Note, however, despite this crowding the nitrogen atom can coordinate to the metal as seen in **3c**.

Mechanistic Studies of CO Insertion into the Pd−Me Bond in Complex 3c. The reaction of the complexes **3a**−**3e** with CO was monitored by ^{1}H NMR spectroscopy. Treatment of neutral palladium complexes **3a**−**3e** with ^{13}CO in CD_2Cl_2 or chlorobenzene-d_5 at ambient temperature or 60 °C cleanly generates the corresponding palladium acyl species. The methyl group of the acyl appears as a doublet resonance around 2.7 ppm (23 °C in CD_2Cl_2) in the ^{1}H NMR spectrum due to ^{13}C−^{1}H splitting [J = 6.4 Hz]. The formation of acyl compounds was confirmed by the proton-coupled ^{13}C NMR, in which the labeled acyl carbon appears as a quartet at ∼231 ppm (23 °C in CD_2Cl_2).

There are two possible pathways for the formation of the acyl species through CO insertion (Scheme 4). The first pathway involves a four-coordinated species: formation of a T-shaped three-coordinate species by dissociation of the coordinated imine, followed by the coordination of CO, migratory insertion, and the re-coordination of the imine. The other possible pathway is through a five-coordinated species: coordination of CO forming the pyramidal structure, followed by migratory insertion. To distinguish between these two mechanisms, the kinetics of the reaction was monitored by following the disappearance of the Pd-CH_3 resonance and/or the appearance of the corresponding Pd-C(O)-Me resonance in the ^{1}H NMR spectrum in CD_2Cl_2 over time. The first-order rate constants and the corresponding enthalpy and entropy of activation for carbon mon-

Table 1. Selected Bond Distances (Å) and Angles (deg) for 3a

Pd1−N2	1.989(10)	N4−C45	1.281(13)
Pd1−C12	2.035(10)	N4−C44	1.397(14)
Pd1−N1	2.038(9)	N1−C7	1.299(14)
Pd1−O2	2.051(7)	N1−C21	1.414(14)
Pd2−N3	1.978(10)	N2−C14	1.283(14)
Pd2−C52	2.010(12)	N2−C13	1.525(12)
Pd2−N4	2.060(9)	O1−C33	1.308(11)
Pd2−O1	2.090(7)	N3−C39	1.307(14)
O2−C1	1.275(13)	N3−C53	1.489(12)
N2−Pd1−C12	87.0(4)	C45−N4−C44	120.9(10)
N2−Pd1−N1	178.6(5)	C45−N4−Pd2	127.4(8)
C12−Pd1−N1	94.1(4)	C44−N4−Pd2	111.7(7)
N2−Pd1−O2	87.4(3)	C7−N1−C21	119.6(9)
C12−Pd1−O2	174.4(4)	C7−N1−Pd1	120.7(7)
N1−Pd1−O2	91.4(3)	C21−N1−Pd1	119.6(7)
N3−Pd2−C52	93.5(4)	C14−N2−C13	116.3(10)
N3−Pd2−N4	178.4(5)	C14−N2−Pd1	129.7(8)
C52−Pd2−N4	87.3(4)	C13−N2−Pd1	113.9(7)
N3−Pd2−O1	91.4(3)	C33−O1−Pd2	125.8(6)
C52−Pd2−O1	175.0(4)	C39−N3−C53	113.0(9)
N4−Pd2−O1	87.8(3)	C39−N3−Pd2	125.0(7)
C1−O2−Pd1	131.0(7)	C53−N3−Pd2	121.9(7)

Table 2. Selected bond distances (Å) and angles (deg) for 3c

Pd1−C12	2.026(3)	O1−C1	1.285(3)
Pd1−N1	2.0314(19)	N5−C67	1.302(3)
Pd1−N2	2.059(2)	N5−C71	1.449(3)
Pd1−O1	2.0990(16)	N6−C82	1.277(3)
Pd2−N3	2.0272(19)	N6−C102	1.521(3)
Pd2−C52	2.023(2)	O3−C61	1.284(3)
Pd2−N4	2.071(2)	N2−C25	1.282(3)
Pd2−O2	2.0944(16)	N2−C92	1.517(3)
Pd3−N5	2.0234(19)	O2−C32	1.285(3)
Pd3−C89	2.028(2)	N4−C53	1.280(3)
Pd3−N6	2.066(2)	N4−C60	1.515(3)
Pd3−O3	2.0950(16)	N3−C38	1.299(3)
N1−C7	1.294(3)	N3−C43	1.453(3)
N1−C13	1.451(3)		
C12−Pd1−N1	93.36(9)	C13−N1−Pd1	123.47(15)
C12−Pd1−N2	88.82(9)	C1−O1−Pd1	128.26(15)
N1−Pd1−N2	177.68(8)	C67−N5−C71	113.35(19)
C12−Pd1−O1	175.50(9)	C67−N5−Pd3	122.30(16)
N1−Pd1−O1	91.08(7)	C71−N5−Pd3	124.08(14)
N2−Pd1−O1	86.74(7)	C82−N6−C102	116.6(2)
N3−Pd2−C52	92.45(9)	C82−N6−Pd3	123.31(18)
N3−Pd2−N4	178.13(8)	C102−N6−Pd3	120.04(15)
C52−Pd2−N4	89.28(9)	C61−O3−Pd3	128.19(14)
N3−Pd2−O2	91.05(7)	C25−N2−C92	117.3(2)
C52−Pd2−O2	176.50(9)	C25−N2−Pd1	123.13(18)
N4−Pd2−O2	87.22(7)	C92−N2−Pd1	119.58(15)
N5−Pd3−C89	92.45(9)	C32−O2−Pd2	128.42(15)
N5−Pd3−N6	176.09(8)	C53−N4−C60	116.1(2)
C89−Pd3−N6	89.05(9)	C53−N4−Pd2	123.94(18)
N5−Pd3−O3	91.28(7)	C60−N4−Pd2	119.98(15)
C89−Pd3−O3	176.08(9)	C38−N3−C43	113.00(19)
N6−Pd3−O3	87.31(7)	C38−N3−Pd2	122.37(16)
C7−N1−C13	114.01(19)	C43−N3−Pd2	124.59(15)
C7−N1−Pd1	122.43(16)		

Table 3. Selected Bond Distances (Å) and Angles (deg) for 3d

Pd1−C21	2.009(9)	N1−C12	1.405(11)
Pd1−N1	2.024(8)	N3−C48	1.332(9)
Pd1−N2	2.048(4)	N3−C49	1.499(10)
Pd1−O1	2.105(6)	O2−C38	1.303(10)
Pd2−N3	1.992(6)	O1−C1	1.275(11
Pd2−O2	2.048(7)	N2−C28	1.289(6)
Pd2−C58	2.075(10)	N2−C22	1.511(9)
Pd2−N4	2.096(5)	C59−N4	1.567(10)
N1−C7	1.267(11)	C65−N4	1.245(7)
C21−Pd1−N1	94.7(3)	C7−N1−Pd1	122.4(6)
C21−Pd1−N2	85.7(3)	C12−N1−Pd1	119.0(6)
N1−Pd1−N2	165.9(2)	C48−N3−C49	112.0(6)
C21−Pd1−O1	173.3(3)	C48−N3−Pd2	124.0(5)
N1−Pd1−O1	91.9(3)	C49−N3−Pd2	123.7(5)
N2−Pd1−O1	87.7(2)	C38−O2−Pd2	132.7(5)
N3−Pd2−O2	90.8(3)	C1−O1−Pd1	124.4(5)
N3−Pd2−C58	93.3(4)	C28−N2−C22	114.4(5)
O2−Pd2−C58	175.9(4)	C28−N2−Pd1	128.7(4)
N3−Pd2−N4	170.0(2)	C22−N2−Pd1	116.9(4)
O2−Pd2−N4	87.3(2)	C65−N4−C59	115.4(6)
C58−Pd2−N4	88.7(3)	C65−N4−Pd2	119.1(5)
C7−N1−C12	118.3(7)	C59−N4−Pd2	125.4(5)

oxide insertion into the Pd(II)−Me bond for **3c** in the absence or presence of benzylidene-*tert*-butylamine are listed in Table 7. It is clear that the presence of an excess imine has little effect on the rate of the reaction. The lack of inhibition by the addition of imine, together with a significant negative activation entropy, suggests that CO insertion proceeds through a five-coordinate intermediate (route 2, Scheme 4).

Insertion of Imine into the Pd−Acyl Bond. Reaction of the title complexes **3a**−**e** with excess imine in the presence of ^{13}CO in chlorobenzene-d_5 was monitored by ^1H, $^{13}C\{^1H\}$, and proton-coupled ^{13}C NMR spectroscopy. The insertion of CO into the Pd−Me bond to form the corresponding acyl compound was observed at ambient temperature (compound **5**, Scheme 4, carbonyl resonance ∼231 ppm).

Warming the reaction mixture to 40 °C resulted in the formation of a new species with a carbonyl resonance at ∼214 ppm. The concentration of this species is gradually increased at the expense of the acyl compound. To rule out the possibility that the resonance at 214 ppm was due to an isomeric acyl species, complex **6** incorporating the symmetrical bidentate ligand [2-[(2,6-

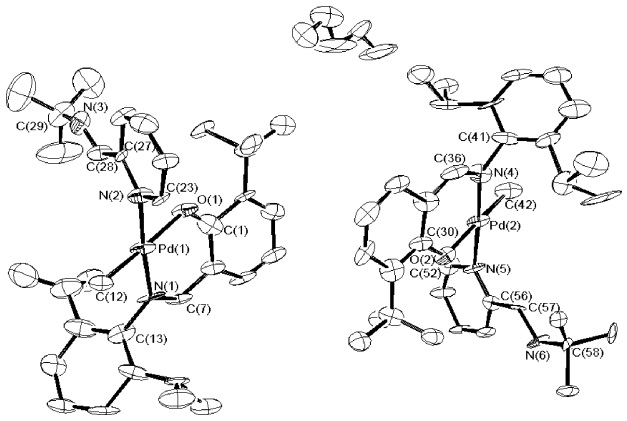

Figure 5. ORTEP view of complex **4**. Hydrogen atoms are omitted for clarity.

Table 4. Selected Bond Distances (Å) and Angles (deg) for 3e

O1−C7	1.280(3)	N1−C1	1.296(3)
O1−Pd1	2.0880(16)	N1−C12	1.447(3)
Pd1−N1	2.0126(18)	N2−C25	1.280(3)
Pd1−C24	2.020(3)	N2−C32	1.468(3)
Pd1−N2	2.0386(19)		
C7−O1−Pd1	128.02(14)	C1−N1−C12	113.94(18)
N1−Pd1−C24	92.89(9)	C1−N1−Pd1	122.46(15)
N1−Pd1−N2	178.87(7)	C12−N1−Pd1	123.58(15)
C24−Pd1−N2	88.08(9)	C25−N2−C32	117.1(2)
N1−Pd1−O1	91.64(7)	C25−N2−Pd1	127.01(17)
C24−Pd1−O1	175.39(8)	C32−N2−Pd1	115.89(15)
N2−Pd1−O1	87.40(7)		

Table 5. Selected Bond Distances (Å) and Angles (deg) for 4

Pd1−N2	2.023(10)	N5−C52	1.368(18)
Pd1−C12	2.029(17)	N4−C36	1.29(2)
Pd1−N1	2.039(11)	N4−C41	1.433(19)
Pd1−O1	2.069(12)	N1−C7	1.264(18)
Pd2−N4	1.981(11)	N1−C13	1.46(2)
Pd2−C42	2.017(19)	O2−C30	1.316(14)
Pd2−N5	2.073(11)	O1−C1	1.23(2)
Pd2−O2	2.084(12)	N3−C28	1.149(16)
N2−C23	1.323(14)	N3−C29	1.500(18)
N2−C27	1.364(16)	N6−C57	1.303(15)
N5−C56	1.339(16)	N6−C58	1.485(15)
N2−Pd1−C12	89.2(5)	C27−N2−Pd1	124.8(8)
N2−Pd1−N1	174.7(6)	C56−N5−C52	119.0(12)
C12−Pd1−N1	95.3(6)	C56−N5−Pd2	120.8(9)
N2−Pd1−O1	85.2(5)	C52−N5−Pd2	119.5(9)
C12−Pd1−O1	174.2(6)	C36−N4−C41	115.2(13)
N1−Pd1−O1	90.2(5)	C36−N4−Pd2	118.4(10)
N4−Pd2−C42	91.3(6)	C41−N4−Pd2	126.4(12)
N4−Pd2−N5	177.5(5)	C7−N1−C13	115.5(12)
C42−Pd2−N5	89.4(6)	C7−N1−Pd1	126.9(11)
N4−Pd2−O2	92.0(5)	C13−N1−Pd1	117.6(10)
C42−Pd2−O2	176.6(6)	C30−O2−Pd2	128.6(9)
N5−Pd2−O2	87.2(4)	C1−O1−Pd1	123.5(10)
C23−N2−C27	117.3(11)	C28−N3−C29	127.0(13)
C23−N2−Pd1	117.8(8)	C57−N6−C58	119.1(12)

Table 6. Crystallographic Data and Data Collection Parameters for Complexes 3a−e and 4

	3a	3c	3d	3e	4
formula	$C_{32}H_{42}N_2OPd$	$C_{105}H_{144}N_6O_3Pd_3$	$C_{74}H_{88}N_4O_2Pd_2$	$C_{38}H_{46}N_2OPd$	$C_{34}H_{47}N_3OPd$
mol wt	577.08	1857.46	1278.28	653.17	620.18
temp (K)	98(2)	98(2)	98(2)	218(2)	98(2) K
wavelength (Å)	0.71073	0.71073	0.71073	0.71073	0.71073 Å
cryst syst	triclinic	monoclinic	triclinic	triclinic	triclinic
space group	$P\bar{1}$	$P2(1)/c$	$P\bar{1}$	$P\bar{1}$	$P\bar{1}$
a (Å)	11.1653(17)	11.4483(11)	11.9939(16)	9.6685(4)	10.895(2)
b (Å)	11.3688(17)	19.4368(19)	12.1298(16)	13.0421(6)	13.620(3)
c (Å)	13.611(2)	43.765(4)	13.9255(18)	14.8920(7)	13.959(3)
α (deg)	105.623(2)	90	82.955(2)	71.6700(10)	64.930(3)
β (deg)	99.448(2)	90	69.190(2)	81.2500(10)	71.179(3)
γ (deg)	113.062(2)	90	60.381(2)	71.0830(10)	73.707(3)
volume (Å^3)	1458.3(4)	9738.5(17)	1642.8(4)	1683.65(13)	1750.8(6)
Z	2	4	2	2	2
F(000)	604	3912	668	684	694
$R(F)$	0.0207	0.0384	0.0164	0.0364	0.0263
$R_w(F)$	0.0586	0.0358	0.0532	0.0937	0.0849
D_{calcd}(g/cm$^{3)}$	1.314	1.267	1.292	1.288	1.245

Scheme 3

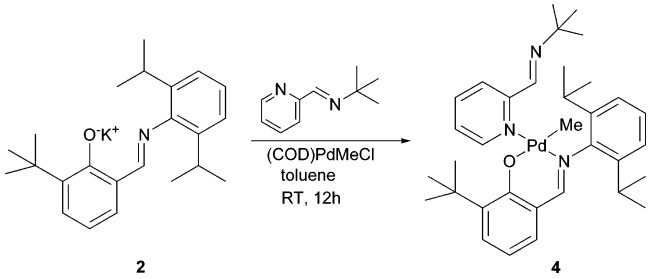

Table 7. Kinetic Data for Insertion of CO into Pd(II)−Me Bond in Complex 3c

	T (K)	k (×10^4 s^{-1})	$\Delta H^{\ddagger}$ (kcal/mol)	$\Delta S^{\ddagger}$ (cal/K·mol)
no imine	273.99	0.075	19.0	−12.5
	286.42	0.25		
50 equiv imine	273.99	0.079	14.7	−28.1
	286.42	0.20		

Table 8. Selected Bond Distances (Å) and Angles (deg) for 6

Pd1−N1	2.0432(12)	N1−C1	1.335(2)
Pd1−N3	2.0550(13)	N1−C6	1.4398(19)
Pd1−N2	2.1380(12)	N2−C3	1.3192(19)
Pd1−C44	2.0423(17)	N2−C18	1.4368(18)
N3−C30	1.4925(19))	N3−C37	1.281(2)
C44−Pd1−N1	91.87(6)	C44−Pd1−N3	81.11(6)
N2−Pd1−N1	91.83(5)	N3−Pd1−N2	95.33(5)
N1−Pd1−N3	172.29(5)	C44−Pd1−N2	175.53(6)

diisopropylphenyl)amino]-4-[(2,6-diisopropylphenyl)imino]pent-2-ene, (2,6-di-^{i}Pr-C_6H_3)-N=C(CH_3)-CH=C(CH_3)-NH-(2,6-di-^{i}Pr-C_6H_3), and *N*-benzylbenzylideneimine, Ph-CH=N-CH_2-Ph, were prepared and utilized (Figure 6, for crystal data see Tables 8 and 9). Figure 7 shows part of the proton-coupled ^{13}C NMR (C_6D_5Cl) spectrum observed in the reaction of **6** with ^{13}CO and PhCH=NCH_2Ph at 50 °C. The quartet at the peak at 231.1 ppm corresponds to the acyl carbon formed by CO insertion into the Pd−Me bond. The simple quartet at 168.7 ppm can be ascribed to the carbonyl resonance of the species formed by imine insertion into the Pd−acyl bond, as has been reported previously (species **7**, Scheme 5).[26,27]

(26) Kacker, S.; Kim, J. S.; Sen, A. *Angew. Chem., Int. Ed.* **1998**, *37*, 1251−1253.

(27) Dghaym, R. D.; Yaccato, K. J.; Arndtsen, B. A. *Organometallics* **1998**, *17*, 4−6.

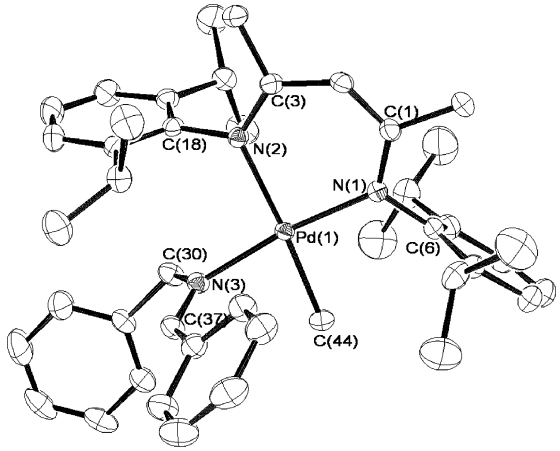

Figure 6. ORTEP view of complex **6**. Hydrogen atoms are omitted for clarity.

Table 9. Crystallographic Data and Data Collection Parameters for Complexes 6

formula	$C_{44}H_{57}N_3Pd$
mol wt	734.33
temp (K)	150(2)
wavelength (Å)	0.71073
cryst syst	monoclinic
space group	$P2(1)/c$
a (Å)	8.8271(4)
b (Å)	19.8265(10)
c (Å)	22.4034(11)
α (deg)	90
β (deg)	94.9130(10)
γ (deg)	90
volume (Å^3)	3906.4(3)
Z	4
F(000)	1552
$R(F)$	0.0256
$R_w(F)$	0.0677
D_{calcd} (g/cm^3)	1.249

However, this reaction is not clean, as evidenced by the other resonances including a ketone-like carbonyl resonance at 214.4 ppm. Unfortunately, our inability to isolate and characterize the formed products has stymied further understanding of the reaction.

Polymerization of Polar or Nonpolar Vinyl Monomers. Polymerization of nonpolar vinyl monomers, such as ethene, propene, or norbornene, using the complexes **3a−e** or **4** was unsuccessful. Presumably this is due to the failure of the coordinated imine to dissociate and provide a vacant coordination site for the incoming

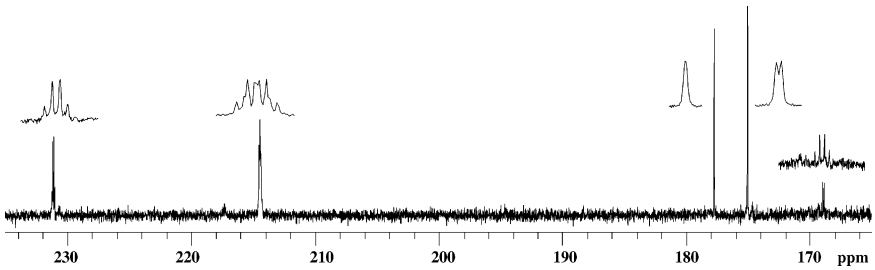

Figure 7. Part of the proton-coupled ^{13}C NMR (C_6D_5Cl) spectrum observed in the reaction of **6** with ^{13}CO and PhCH=NCH_2Ph.

Scheme 4

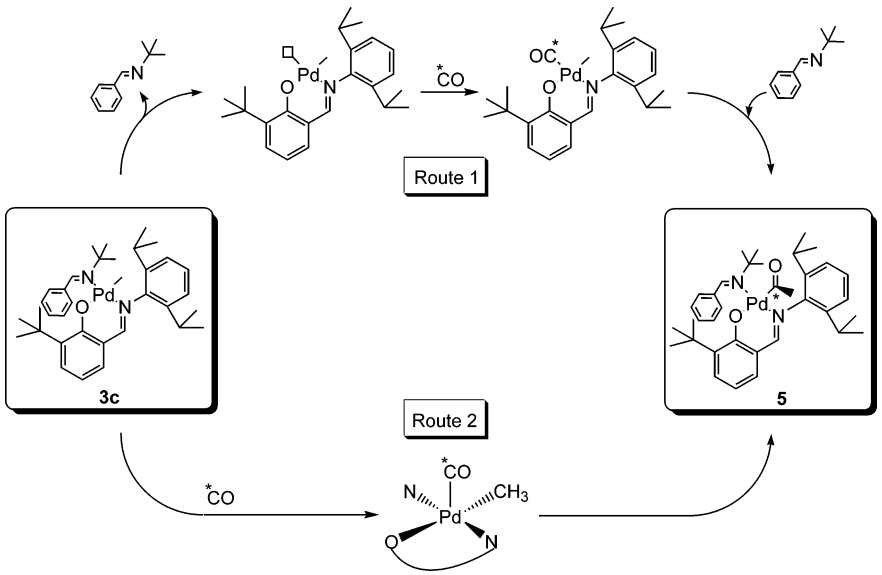

Scheme 5. Proposed Imine Insertion Pathway

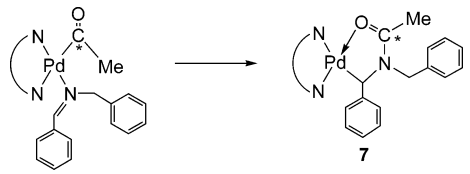

Table 10. Polymerization of Methyl Acrylate Using Complexes 3a−e and 4[a]

entry	catalyst	time (h)	yield (g)	M_n ($\times 10^{-3}$)[c]	M_w/M_n[c]
1	**3a**	3	1.1	211	1.78
2	**3b**	3	1.1	970	6.74
3	**3c**	3	1.1	1584	5.83
4	**3d**	3	1.7	1616	5.85
5[b]	**3d**	3	2.9	346	2.14
6	**3e**	3	2.0		
7	**4**	3	0.7	612	3.10

[a] Reaction conditions: Pd complex (3.1×10^{-5} mol), MA (8 g), chlorobenzene (6 mL), ambient temperature. [b] In chlorobenzene (30 mL). [c] Molecular weight determined by GPC versus polystyrene standards with chloroform as eluent.

monomer. The observation that CO insertion proceeds without imine dissociation (Scheme 4, route 2) supports this hypothesis.

Polymerization of methyl acrylate using catalysts **3a**−**e** or **4** was carried out in chlorobenzene at ambient temperature (Table 10). Low to moderate yields of poly(methyl acrylate) were obtained at the condition indicated. The polymers produced have high (M_n > 211 000) to ultrahigh (M_n > 1 600 000) molecular weight and showed high polydispersity index in general. An important reason for high polydispersity is that the rapid increase in solution viscosity prevented effective stirring. Indeed, decreasing the monomer concentration by increasing the amount of solvent from 6 mL to 30 mL gave a higher polymer yield with a narrower polydispersity (entry 4 versus 5).

One focus of this study was the possible application of the palladium-based neutral complexes as catalysts for the vinyl insertion polymerization of polar or nonpolar vinyl monomers. Recently, Sen[24] as well as Novak and co-workers[23] reported on the homopolymerization of methyl acrylate using neutral palladium compounds where a radical mechanism was invoked. Complexes **3a**−**e** or **4** failed to initiate the polymerization of methyl methacrylate or styrene, two other monomers that are readily polymerized by a radical pathway. However, the polymerization of methyl acrylate by **3a**−**e** or **4** was completely halted upon addition of the radical trap, galvinoxyl, to the reaction mixture. Thus, a radical (albeit "nontraditional") pathway appears to be operative, although there has been "a warning on the use of radical traps as a test for radical mechanisms".[28]

In conclusion, we have synthesized a serious of neutral salicylaldiminato Pd(II) complexes: Pd(Me)(Ph-CH=N−R′)[3-^{t}Bu-2-(O)C_6H_3-CH=N-2,6-di-^{i}Pr−C_6H_3] (R = CH_3, *n*-Pr, *tert*-Bu, Ph, benzyl) (**3a**−**3e**) and Pd(Me)-[2-(CH=N-*t*-Bu)-Py][3-^{t}Bu-2-(O)C_6H_3-CH=N-2,6-di-^{i}Pr-C_6H_3] (**4**). These complexes have been isolated and characterized spectroscopically, and the solid-state struc-

(28) Albeniz, A. C.; Espinet, P.; Lopez-Fernandez, R.; Sen, A. *J. Am. Chem. Soc.* **2002**, *124*, 11278−11279.

tures of the complexes have also been characterized by X-ray single-crystal structure analysis. According to the results of the NMR studies, the complexes react with carbon monoxide to form corresponding acyl complexes through a five-coordinated intermediate. The acyl compounds in turn undergo imine insertion. The neutral complexes show moderate catalytic activity for the polymerization of methyl acrylate at ambient temperature, producing polymers with a high molecular weight but broad polydispersity index. The complexes are unreactive toward insertion polymerization of alkenes presumably because of the inability of the coordinate imine (or pyridine) to undergo ready displacement by an incoming substrate. Efforts to synthesize more substitutionally labile complexes are underway.

Experimental Section

Generation Considerations. All syntheses and manipulations of air- and moisture-sensitive compounds were carried out in flame-dried Schlenk-type glassware on a dual-manifold Schlenk line, on a high vacuum with argon line, or in a nitrogen-filled glovebox.

Nuclear magnetic resonance (NMR) spectra were recorded on a Bruker DRX 400 NMR spectrometer, DPX 300 NMR spectrometer, and CDPX 300 NMR spectrometer. Splitting patterns are designated as follows: s, singlet; bs, broad singlet; d, doublet; dd, doublet of doublets; t, triplet; td, triplet of doublets; sept, septet; m, multiplet. All ^{1}H NMR spectra are reported in δ units, parts per million (ppm) downfield from tetramethylsilane. All ^{13}C NMR spectra are reported in ppm relative to tetramethylsilane using CD_2Cl_2, toluene-d_8, or chlorobenzene-d_5 as an internal standard. Variable-temperature ^{1}H NMR experiments were performed on a Bruker DPX 300 NMR spectrometer, using CD_2Cl_2, toluene-d_8, or chlorobenzene-d_5 as solvent. Actual NMR probe temperatures were measured using anhydrous methanol (with 0.03% concentrated HCl) or ethylene glycol (neat) in a 5 mm NMR tube. NMR analyses of polymers were performed on a Bruker DPX 300 NMR spectrometer at ambient or elevated temperature, using $CDCl_3$, chlorobenzene-d_5, dichlorobenzene-d_4, or tetrachloroethane-d_2 as solvent unless otherwise noted.

Size exclusion chromatography data were obtained on a Shimadzu SEC System using a three-column bank (Styragel 7.8 × 300 mm columns, 100−5000 D, 500−30 000 D, 2000−4 000 000 D), a Shimadzu RID-10A differential refractometer, and a Shimadzu LC-10AT pump/controller. Size exclusion chromatography was performed in chloroform at ambient temperature and calibrated to polystyrene standards.

Chlorobenzene and dichloromethane was obtained from Aldrich and dried via passage over a column of activated alumina (LaRoche A-2).[29] Toluene and diethyl ether were deoxygenated and dried via passage over a column of activated alumina (LaRoche A-2) and columns of Engelhard CU-0226S.[29] Pentane and tetrahydrofuran were distilled under nitrogen from sodium benzophenone ketyl. All solvents were degassed by repeated freeze−pump−thaw cycles and stored over 4 Å molecular sieves under nitrogen. Norbornene was purchased from Acros Organics and used without further purification. Methyl acrylate and methyl methacrylate were purchased from Aldrich and used after repeated freeze−pump−thaw cycles prior to use. (1,5-Cyclooctadien)palladium(methyl)(chloride), [(COD)Pd(Me)(Cl)], was prepared as previously reported.[25]

3-^{t}Bu-2-(OH)C_6H_3-CH=N-2,6-di-^{i}Pr−C_6H_3 (1). To 3-*tert*-butyl-2-hydroxybenzaldehyde (1 g, 5.6 mmol) in methanol (50 mL) was added 2,6-diisopropylaniline (1.5 g, 8.4 mmol), followed a catalytic amount of formic acid (2 drops). The solution was stirred at room temperature for 12 h. Removal of solvent in vacuo yielded a yellow oil. Residual 2,6-diisopropylaniline was further removed by vacuum distillation, giving a yellow oily product that solidified upon cooling. ^{1}H NMR ($CDCl_3$) (ppm): 13.65 (br, 1H, −O*H*), 8.35 (s, 1H, −C*H*=N−), 7.49−6.91 (m, 6H, Ar-*H*), 3.06 (sept, 2H, −C*H*$(CH_3)_2$), 1.52 (s, 9H, −C(C*H*$_3)_3$), 1.22 (d, 12H, −CH(C*H*$_3)_2$). ^{13}C NMR ($CDCl_3$) (ppm): 167.96 (−*C*H=N−), 160.99, 146.72, 139.31, 137.95, 131.08, 130.78, 125.70, 123.57, 118.96, 118.60 (Ar), 35.22 (−*C*Me$_3$), 29.51 (−C(*C*H$_3)_3$), 28.49 (−*C*H$(CH_3)_2$), 23.73 (−CH-(*C*H$_3)_2$).

[3-^{t}Bu-2-(OK)C_6H_3-CH=N-2,6-di-^{i}Pr−C_6H_3]·THF (2). To a stirred suspension of KH (0.19 g, 4.68 mmol) in THF (30 mL) was added ligand **1** (0.79 g, 2.34 mmol) in THF (20 mL) at room temperature. The reaction mixture was stirred for 2 h and filtered to remove excess KH. After removing solvent under vacuum, a small amount of pentane was added to dissolve starting material. Upon filtering and washing with pentane, the potassium salt THF adduct was obtained as a yellow solid. Yield: 0.97 g, 92%.

Pd(Me)(Ph-CH=N-CH$_3$)[3-^{t}Bu-2-(O)C_6H_3-CH=N-2,6-di-^{i}Pr-C_6H_3] (3a). To a mixture of [3-^{t}Bu-2-(OK)C_6H_3-CH=N-2,6-di-^{i}Pr-C_6H_3]·THF (0.42 g, 0.94 mmol) and Ph-CH=N-CH$_3$ (0.11 g, 0.94 mmol) in toluene (30 mL) was added (COD)PdMeCl (0.25 g, 0.94 mmol) in toluene (10 mL). The reaction mixture was stirred for 12 h and was filtered to remove a small quantity of dark insoluble material. The solvent was removed in vacuo to yield a yellow solid. Recrystallization from pentane gave a yellow crystalline solid, which was suitable for X-ray crystal structure analysis. Yield: 0.49 g, 91%. ^{1}H NMR (CD_2Cl_2) (ppm): 8.36 (s, 1H, Pd-O-Ar-C*H*=N−), 7.74 (s, 1H, Ph-C*H*=N-CH$_3$), 8.98 (d), 7.58−7.49 (m), 7.28 (dd), 7.21−7.16 (dd), 7.00 (dd), 6.35 (t) (11H, Ar-H), 3.99 (s, 3H, Ph-CH=N-C*H*$_3$) 3.55, 3.22 (hept each, 2H, Ar-C*H*$(CH_3)_2$), 1.29 (s, 9H, Ar-C(C*H*$_3)_3$), 1.38, 1.24, 1.18, 1.16 (d each, 12H, Ar-CH(C*H*$_3)_2$), −0.49 (s, 3H, Pd-C*H*$_3$). ^{13}C NMR (CD_2Cl_2) (ppm): 167.7 (Pd-O-Ar-*C*H=N−), 166.1 (Ph-*C*H=N-CH$_3$), 141.6, 141.5, 134.9, 132.4, 131.3, 130.7, 129.1, 128.9, 128.6, 128.5, 126.4, 123.5, 119.9, 112.0 (Ar), 53.4 (Ph-CH=N-*C*H$_3$) 35.4 (Ar-*C*$(CH_3)_3$), 29.5 (Ar-C(*C*H$_3)_3$), 28.0 (Ar-*C*H$(CH_3)_2$), 25.2, 25.0, 23.0, 22.7 (Ar-CH(*C*H$_3)_2$), −5.6 (Pd-*C*H$_3$).

Pd(Me)(Ph-CH=N−CH$_2$-CH$_2$-CH$_3$)[3-^{t}Bu-2-(O)C_6H_3-CH=N-2,6-di-^{i}Pr-C_6H_3] (3b). To a mixture of [3-^{t}Bu-2-(OK)C_6H_3-CH=N-2,6-*di*-^{i}Pr-C_6H_3]·THF (0.42 g, 0.94 mmol) and Ph-CH=N-CH$_2$-CH$_2$-CH$_3$ (0.14 g, 0.94 mmol) in toluene (30 mL) was added (COD)PdMeCl (0.25 g, 0.94 mmol) in toluene (10 mL). The reaction mixture was stirred for 12 h and then was filtered to remove a small quantity of dark insoluble material. The solvent was removed in vacuo to yield a yellow solid. Recrystallization from pentane gave a yellow crystalline solid, which was suitable for X-ray crystal structure analysis. Yield: 0.51 g, 89%. ^{1}H NMR (CD_2Cl_2) (ppm): 8.38 (s, 1H, Pd-O-Ar-C*H*=N−), 7.70 (s, 1H, Ph-C*H*=N-CH$_2$-Ph), 8.93 (d), 7.54−7.43 (m), 7.24 (dd), 7.17−7.12 (m), 6.96 (dd), 6.31 (t) (11H, Ar-*H*), 4.33, 3.68 (m each, 2H, Ph-CH=N-C*HH*-CH$_2$-CH$_3$), 3.64, 3.39 (hept, 2H, Ar-C*H*$(CH_3)_2$), 2.31 (sext, 2H, N-CH$_2$-C*H*$_2$-CH$_3$), 1.25 (s, 9H, Ar-C(C*H*$_3)_3$), 1.34, 1.21, 1.15, 1.12 (d each, 12H, Ar-CH-(C*H*$_3)_2$), 1.02 (Ph-CH=N−CH$_2$-CH$_2$-C*H*$_3$), −0.62 (s, 3H, Pd-C*H*$_3$). ^{13}C NMR (CD_2Cl_2) (ppm): 167.0 (Pd-O-Ar-*C*H=N−), 166.0 (Ph-*C*H=N-CH$_2$-CH$_2$-CH$_3$), 148.7, 141.5, 141.4, 135.0, 134.2, 132.3, 131.4, 130.7, 128.5, 126.3, 124.5, 123.5, 123.4, 120.0, 112.0 (Ar), 68.6 (Ph-CH=N-*C*H$_2$-CH$_2$-CH$_3$), 35.3 (Ar-*C*$(CH_3)_3$) 29.5 (Ar-C(*C*H$_3)_3$), 28.1, 28.0 (Ar-*C*H$(CH_3)_2$), 25.0 (Ph-CH=N-CH$_2$-*C*H$_2$-CH$_3$), 25.3, 25.1, 23.1, 22.6 (Ar-CH(*C*H$_3)_2$), 11.8 (Ph-CH=N−CH$_2$-CH$_2$-*C*H$_3$), −5.0 (Pd-*C*H$_3$).

Pd(Me)(Ph-CH=N-*t*-Bu)[3-^{t}Bu-2-(O)C_6H_3-CH=N-2,6-di-^{i}Pr-C_6H_3] (3c). To a mixture of [3-^{t}Bu-2-(OK)C_6H_3-CH=N-2,6-di-^{i}Pr-C_6H_3]·THF (0.42 g, 0.94 mmol) and Ph-CH=N-t-Bu (0.15 g, 0.94 mmol) in toluene (30 mL) was added (COD)PdMeCl (0.25 g, 0.94 mmol) in toluene (10 mL). The reaction mixture was stirred for 12 h and then filtered to remove a small

(29) Pangborn, A. B.; Giardello, M. A.; Grubbs, R. H.; Rosen, R. K.; Timmers, F. J. *Organometallics* **1996**, *15*, 1518−1520.

quantity of dark insoluble material. The solvent was removed in vacuo to yield a yellow solid. Recrystallization from pentane at −25 °C gave a yellow crystalline solid, which was suitable for X-ray crystal structure analysis. Yield: 0.52 g, 90%. ^{1}H NMR (CD_2Cl_2) (ppm): 8.51 (s, 1H, Pd-O-Ar-C*H*=N−), 7.69 (s, 1H, Ph-C*H*=N-*t*-Bu), 8.92 (d), 7.52−7.43 (m), 7.25 (dd), 7.15−7.07 (m), 6.95 (dd), 6.31 (t) (11H, Ar-*H*), 3.69, 3.21 (hept each, 2H, Ar-C*H*(CH_3)$_2$), 1.76 (s, 9H, −N-C(C*H*$_3$)$_3$), 1.29 (s, 9H, Ar-C(C*H*$_3$)$_3$), 1.24, 1.12, 1.10, 1.03 (d each, 12H, Ar-CH(C*H*$_3$)$_2$), −0.66 (s, 3H, Pd-C*H*$_3$). ^{13}C NMR(CD_2Cl_2) (ppm): 169.1 (Pd-O-Ar-*C*H=N−), 166.2 (Ph-*C*H=N-t-Bu), 148.8, 141.6, 141.5, 135.9, 135.1, 131.9, 131.4, 130.4, 128.3, 126.2, 123.5, 123.3, 120.0, 111.8(Ar), 64.7 (−N-*C*(CH_3)$_3$), 35.4 (Ar-*C*(CH_3)$_3$), 32.1 (−N-C(*C*H$_3$)$_3$), 29.7 (Ar-C(*C*H$_3$)$_3$), 28.0, 27.9 (Ar-*C*H(CH_3)$_2$), 25.3, 25.1, 23.0, 22.8 (Ar-CH(*C*H$_3$)$_2$), −6.01 (Pd-*C*H$_3$).

Pd(Me)(Ph-CH=N-Ph)[3-^{t}Bu-2-(O)C_6H_3-CH=N-2,6-di-^{i}Pr-C_6H_3] (3d). To a mixture of [3-^{t}Bu-2-(OK)C_6H_3-CH=N-2,6-di-^{i}Pr-C_6H_3]·THF (0.42 g, 0.94 mmol) and Ph-CH=N-Ph (0.17 g, 0.94 mmol) in toluene (30 mL) was added (COD)PdMeCl (0.25 g, 0.94 mmol) in toluene (10 mL). The reaction mixture was stirred for 12 h and then was filtered to remove a small quantity of dark insoluble material. The solvent was removed in vacuo to yield a yellow solid. Recrystallization from pentane gave a yellow crystalline solid, which was suitable for X-ray crystal structure analysis. Yield: 0.55 g, 92%. ^{1}H NMR (CD_2Cl_2) (ppm): 8.56 (s, 1H, Pd-O-Ar-C*H*=N−), 7.70 (s, 1H, Ph-C*H*=N-Ph), 9.17 (d), 7.81 (d), 7.61−7.15 (m), 6.95 (d), 6.30 (t) (16H, Ar-*H*), 3.54, 3.47 (hept each, 2H, Ar-C*H*(CH_3)$_2$), 1.13 (s, 9H, Ar-C(C*H*$_3$)$_3$), 1.25, 1.24, 1.16, 1.10 (d each, 12H, Ar-CH(C*H*$_3$)$_2$), −0.47 (s, 3H, Pd-C*H*$_3$). ^{13}C NMR (CD_2Cl_2) (ppm): 168.1 (Pd-O-Ar-*C*H=N−), 166.1 (Ph-*C*H=N-CH_2-Ph), 153.0, 148.7, 141.6, 141.4, 134.8, 133.3, 131.4, 131.3, 129.2, 128.7, 128.0, 126.4, 124.1, 123.6, 119.8, 112.0 (Ar), 35.3 (Ar-*C*(CH_3)$_3$) 29.4 (Ar-C(*C*H$_3$)$_3$), 28.0 (Ar-*C*H(CH_3)$_2$), 25.3, 25.0, 23.0, 22.6 (Ar-CH(*C*H$_3$)$_2$), −4.1 (Pd-*C*H$_3$).

Pd(Me)(Ph-CH=N-CH_2-Ph)[3-^{t}Bu-2-(O)C_6H_3-CH=N-2,6-di-^{i}Pr-C_6H_3] (3e). To a mixture of [3-^{t}Bu-2-(OK)C_6H_3-CH=N-2,6-di-^{i}Pr-C_6H_3]·THF (0.23 g, 0.52 mmol) and Ph-CH=N-CH_2-Ph (0.11 g, 0.56 mmol) in toluene (30 mL) was added (COD)PdMeCl (0.15 g, 0.57 mmol) in toluene (10 mL). The reaction mixture was stirred for 12 h and then was filtered to remove a small quantity of dark insoluble material. The solvent was removed in vacuo to yield a yellow solid. Recrystallization from methylene dichloride and pentane gave a yellow crystalline solid, which was suitable for X-ray crystal structure analysis. Yield: 0.31 g, 92%. ^{1}H NMR (CD_2Cl_2) (ppm): 8.49 (s, 1H, Pd−O-Ar-C*H*=N−), 7.71 (s, 1H, Ph-C*H*=N-CH_2-Ph), 5.61 (d, 1H, Ph-CH=N-C*H*H′-Ph), 5.10 (d, 1H, Ph-CH=N-CH*H*′-Ph), 8.94 (d), 7.65−6.98 (m), 6.37 (t) (16H, Ar-*H*), 3.42 (hept, 2H, Ar-C*H*(CH_3)$_2$), 1.38 (s, 9H, Ar-C(C*H*$_3$)$_3$), 1.22, 1.19, 1.16, 1.11 (d each, 12H, Ar-CH(C*H*$_3$)$_2$), −0.86 (s, 3H, Pd-C*H*$_3$). ^{13}C NMR (CD_2Cl_2) (ppm): 166.9 (Pd-O-Ar-*C*H=N−), 166.3 (Ph-*C*H=N-CH_2-Ph), 148.6, 141.6, 136.4, 135.0, 132.5, 131.5, 130.7, 129.1, 129.0, 128.7, 128.5, 126.3, 123.4, 112.1 (Ar), 69.45 (=N-*C*H$_2$-Ph), 35.4 (Ar-*C*(CH_3)$_3$) 29.7 (Ar-C(*C*H$_3$)$_3$), 27.9 (Ar-*C*H(CH_3)$_2$), 25.2, 23.2 (Ar-CH(*C*H$_3$)$_2$), −4.4 (Pd-*C*H$_3$).

Pd(Me)[2-(CH=N-*t*-Bu)-Py][3-^{t}Bu-2-(O)C_6H_3-CH=N-2,6-di-^{i}Pr−C_6H_3] (4). To a mixture of [3-^{t}Bu-2-(OK)C_6H_3-CH=N-2,6-di-^{i}Pr-C_6H_3]·THF (0.42 g, 0.94 mmol) and 3-(CH=N-*t*-Bu)-Py (0.15 g, 0.94 mmol) in toluene (30 mL) was added (COD)PdMeCl (0.25 g, 0.94 mmol) in toluene (10 mL). The reaction mixture was stirred for 12 h and then was filtered to remove a small quantity of dark insoluble material. The solvent was removed in vacuo to yield a yellow solid. Recrystallization from pentane gave a yellow crystalline solid, which was suitable for X-ray crystal structure analysis. Yield: 0.56 g, 93%. ^{1}H NMR (CD_2Cl_2) (ppm): 9.94 (s, 1H, Pd-O-Ar-C*H*=N−), 7.71 (s, 1H, Py-C*H*=N-*t*-Bu), 8.97 (d), 8.24 (s), 7.87 (t), 7.36 (dt), 7.26−7.14 (m), 6.95 (dd), 6.30 (t) (10H, Ar-H), 3.69, 3.50 (hept each, 2H, Ar-C*H*(CH_3)$_2$), 1.33 (s, 9H, Ar-C(C*H*$_3$)$_3$), 1.02 (s, 9H, =N-C(C*H*$_3$)$_3$), 1.35, 1.16, 1.12 (d each, 12H, Ar-CH(C*H*$_3$)$_2$), −0.26 (s, 3H, Pd-C*H*$_3$). ^{13}C NMR (CD_2Cl_2) (ppm): 166.4 (Ph-*C*H=N-t-Bu), 156.9 (Pd-O-Ar-*C*H=N−), 168.2, 155.9, 152.3, 141.5, 137.7, 134.7, 131.4, 129.4, 128.6, 126.5, 125.2, 123.7, 123.5, 123.1, 119.8, 112.1 (Ar), 58.7 (=N-*C*H(CH_3)$_2$), 35.1 (Ar-*C*H(CH_3)$_2$), 29.5 (Ar-C(*C*H$_3$)$_3$), 29.3 (=N-C(*C*H$_3$)$_3$), 28.3, 28.1 (Ar-*C*H(CH_3)$_2$), 25.0, 22.9 (Ar-CH(*C*H$_3$)$_2$), −4.0 (Pd-*C*H$_3$).

Pd(Me)(Ph-CH=N-CH_2-Ph)[2,6-di-^{i}Pr-C_6H_3-N-C(Me)-CH-C(Me)-N-2,6-di-^{i}Pr-C_6H_3] (6). To a mixture of [2,6-di-^{i}Pr-C_6H_3−N=C(Me)-CH=C(Me)-N(H)-2,6-di-^{i}Pr-C_6H_3]·Tl (0.50 g, 0.8 mmol) and Ph-CH=N-CH_2-Ph (0.15 g, 0.8 mmol) in toluene (30 mL) was added (COD)PdMeCl (0.21 g, 0.8 mmol) in toluene (10 mL). The reaction mixture was stirred for 12 h and then was filtered to remove a small quantity of dark insoluble material. The solvent was removed in vacuo to yield a yellow solid. Recrystallization from methylene dichloride and pentane gave a yellow crystalline solid, which was suitable for X-ray crystal structure analysis. Yield: 0.57 g, 97%. ^{1}H NMR (CD_2Cl_2) (ppm): 7.30 (s, 1H, Ph-C*H*=N−), 9.05 (d), 7.46−7.32 (m), 7.22−6.86 (m), 6.63 (d) (16H, Ar-*H*), 4.68 (s, N−C(CH$_3$)-C*H*-C(CH$_3$)-N), 4.57, 3.29 (d each, 2H, Ph-C*HH*-N), 3.79, 3.66, 3.41, 2.86 (hept each, 4H, Ar-C*H*(CH_3)$_2$, Ar-C*H*(CH_3)$_2$, Ar-C*H*(CH_3)$_2$, Ar-C*H*(CH_3)$_2$), 1.56, 1.53 (s each, 6H, N-C(C*H*$_3$)-CH-C(C*H*$_3$)-N), 1.50, 1.24, 1.20, 1.15, 1.06, 0.84, 1.82, 0.33 (d each, 24H, Ar-CH(C*H*$_3$)$_2$), −0.74 (s, 3H, Pd-C*H*$_3$). ^{13}C DEPT135 NMR (CD_2Cl_2): δ 166.3 (−*C*H=N−), 132.4, 131.5, 129.2, 128.5, 125.0, 124.6, 124.2, 123.4, 123.2 (Ar), 94.5 (−C(CH$_3$)-*C*H-C(CH$_3$)−), 65.9 (Ph-*C*H$_2$-N), 28.4, 28.1, 27.7, 27.4 (Ar-*C*H-(CH_3)$_2$), 26.2 ((−C(*C*H$_3$)-CH-C(*C*H$_3$)−), 25.4, 25.1, 24.9, 24.8, 24.7, 24.2, 24.1, 23.8 (Ar-CH(*C*H$_3$)$_2$), 4.8 (Pd-*C*H$_3$).

General Procedures for Polymerization Reactions. In a drybox under a nitrogen atmosphere, a title complex (3.1×10^{-5} mol) was dissolved in chlorobenzene (6 mL or 30 mL) in a 100 mL Schlenk flask. A specified amount of methyl acrylate was introduced to the flask. The reaction mixture was stirred at the desired temperature. After the specified reaction time, the reaction was quenched with methanol. The precipitated polymer was filtered and washed with methanol. Volatiles were removed from the polymer in vacuo, and the polymer was dried under vacuum overnight.

General Procedure for NMR Experiments. In a drybox under a nitrogen atmosphere, **3c** (1.7×10^{-5} mol) with or without Ph-C=N-*n*-Pr (8.3×10^{-4} mol) was weighed into a high-pressure NMR tube. CD_2Cl_2 (1 mL) was added to the NMR tube. The tube was then capped, removed from the drybox, and cooled to ca. −90 °C. After applying vacuum briefly, the mixture are allowed to reach ambient temperature. The NMR tube was then charged with ^{13}C-labeled carbon monoxide (50 psi) and cooled again to ca. −90 °C using a liquid nitrogen/acetone slurry. The tube was shaken very briefly and transferred to the NMR probe, which was at preset temperature. NMR spectra were acquired every 10 min at the desired temperature.

Acknowledgment. We thank the Department of Energy, Office of Basic Energy Sciences, for funding. We thank NSF (CHE-0131112) for funding the X-ray diffractometer and Dr. Hemant Yennawar for assistance with the X-ray structure determination.

Note Added after ASAP Publication. The compounds **3a**, **3d**, and **4** have been refined in the higher symmetry space group P$\bar{1}$. The updated CIF files now appear in the Supporting Information.

Supporting Information Available: Details of crystal structure determinations, tables of positional parameters for atoms, bond distances and angles, and anisotropic thermal parameters, and CIF files for the crystal structures. This material is available free of charge via the Internet at http://pubs.acs.org.

OM050126A